

Measurement of Conatumumab-Induced Apoptotic Activity in Tumors by Fine Needle Aspirate Sampling

Stephen J. Zoog,¹ Connie Y. Ma,¹ Paula J. Kaplan-Lefko,² Jennifer M. Hawkins,³ Jodi Moriguchi,² Lei Zhou,⁴ Yang Pan,⁵ Cheng-Pang Hsu,⁶ Greg Friberg,⁷ Roy Herbst,⁸ John Hill,⁷ Gloria Juan^{1*}

¹Department of Clinical Immunology, Amgen Inc., Thousand Oaks, California

²Department of Oncology Research, Amgen Inc., Thousand Oaks, California

³Department of Pathology, Amgen Inc., Thousand Oaks, California

⁴Department of Biostatistics, Amgen Inc., Thousand Oaks, California

⁵Department of Molecular Sciences, Amgen Inc., Seattle, Washington

⁶Department of Pharmacokinetics and Drug Metabolism, Amgen Inc., Thousand Oaks, California

⁷Department of Early Development, Amgen Inc., Thousand Oaks, California

⁸Department of Thoracic/Head and Neck Medical Oncology, University of Texas M. D. Anderson Cancer Center, Houston, Texas

Received 19 March 2010; Revision Received 14 May 2010; Accepted 7 June 2010

Additional Supporting Information may be found in the online version of this article.

This study is based in part on a presentation given at the American Association of Pharmaceutical Scientists on June 21–24, 2009, Seattle, WA

Grant sponsor: Amgen Inc.

• Abstract

Conatumumab is a monoclonal antibody specific for death receptor 5 (DR5) that activates caspases leading to DNA fragmentation and tumor-cell death. Like other Tumor Necrosis Factor-Related Apoptosis-Inducing Ligand (TRAIL) receptor therapies, conatumumab is currently being evaluated in clinical trials across a variety of tumor types. However, molecular evidence of on-target drug activity in tumors is often an elusive goal for clinical investigation. Here we evaluated a translational approach using a relevant biopsy method, fine needle aspirates (FNAs), to study the on-target pharmacodynamics of conatumumab pre-clinically. As detected by laser scanning cytometry, drug-induced caspase-3 activation in FNA biopsies of Colo205 xenografts correlated well with activated caspase-3 in conventional section-based samples. Furthermore, in tumor-bearing mice, surrogate assays of serum caspase-3/7 activity and serum drug exposure correlated with in situ caspase-3 activation. We found that one advantage of FNA sampling over other sampling techniques was the ability to measure caspase activity on a per cell basis using DNA content information. To adapt the utility of FNAs for measuring pharmacodynamic markers in humans, detection of activated caspase-3 was multiplexed with EpCAM to characterize mock and clinical FNAs from colorectal and non-small cell lung cancer patients. These data suggest that FNA sampling is a practical method to cytometrically evaluate tumors for pharmacological impact in a clinical setting. © 2010 International Society for Advancement of Cytometry

• Key terms

conatumumab; fine-needle aspirates; apoptosis; caspase-3

TUMOR -necrosis factor-related apoptosis-inducing ligand (TRAIL) binds Death Receptor 4 (DR4; or Trail Receptor 1 [TR-1]) and Death Receptor 5 (DR5; or Trail Receptor 2 [TR-2]) (1–5). Binding of TRAIL to DR4 or DR5 results in oligomerization of the receptors, clustering of their intracellular death domains, and assembly of the death-inducing signaling complex (DISC) (reviewed by Peter and Kramer (6)). Recruitment of cysteinyl aspartate proteases (caspases-8 and -10) to the DISC through FADD results in their proximal activation, followed by proteolytic processing of downstream effector caspases-3, -6, and -7 (7–9). Activated effector caspases cleave various cellular substrates culminating in DNA fragmentation and cell death. Caspase-8 activation by TRAIL may also trigger cleavage of Bid into tBid and thereby amplify the death signal by provoking release of mitochondrial proapoptotic factors (10,11). Although DR4 and DR5 are expressed on tumor and nontumor cells, recombinant TRAIL selectively kills tumor cells (12,13). This characteristic has led to widespread investigation of DR agonists as potential therapies alone or in combination with less-specific cytotoxic therapies.

DR4- or DR5-specific antibodies can mimic the action of TRAIL to trigger death of TRAIL-sensitive cells (14–18). Conatumumab is an investigational, fully human monoclonal (IgG1) antibody agonist of DR5 that induces apoptosis in multiple

*Correspondence to: Gloria Juan, Department of Clinical Immunology, Amgen Inc., One Amgen Center Drive, Thousand Oaks, CA 91320, USA
Email: gjuan@amgen.com

Published online 8 July 2010 in Wiley Online Library
(wileyonlinelibrary.com)

DOI: 10.1002/cyto.a.20940

© 2010 International Society for Advancement of Cytometry

tumor cell types (19). Conatumumab inhibited tumor growth in multiple xenograft models as a single agent and enhanced the antitumor activity of chemotherapy in combination studies. The proapoptotic activity of conatumumab *in vivo* was confirmed by induction of caspases-8, -9, and -3 in excised xenografts. In the first-in-human trial in patients with advanced solid tumors, conatumumab demonstrated evidence of anti-tumor activity (20), and conatumumab is currently being evaluated in a number of clinical trials across a variety of tumor types. We sought to develop a target-tissue biomarker assay that may be used in the clinical setting to provide mechanistic evidence of drug activity.

Fine needle aspiration (FNA) is an inexpensive biopsy technique that is established as a reliable method for diagnosis based on isolated or grouped cells (21,22). Early studies demonstrated that FNA samples are representative of the overall tumor phenotype (23,24). More recently, FNA sampling has been extended to immunocytochemical analysis of signal-transduction intermediates (25,26). Certain features of FNAs, such as small sample volume and intact cellularity, are well suited for quantitative fluorochromatic imaging platforms such as laser scanning cytometry (26–28). However, like other biopsy methods, preanalytical variability of FNA sampling should be addressed prior to clinical implementation for each analyte. Assessments should include compatibility of the analyte with the biopsy procedure, and proof-of-concept experiments designed to support the suitability of FNA sampling for observing pharmacodynamic changes.

In this study, we describe a novel approach to measure activated caspase-3 in tumor cell samples *in situ* using FNAs and laser scanning cytometry. We demonstrate that caspase-3 activation can be directly measured in a whole-cell assay while multiplexing with tumor markers and DNA content information to distinguish tumor cells from stromal cells and other non-tumor cells. We attempted to establish the feasibility of using FNAs and laser scanning cytometry to investigate the pharmacodynamic impact of conatumumab by directly comparing levels of activated caspase-3 in FNAs with levels of activated caspase-3 in tumor sections, serum caspase-3/7 activity, and serum conatumumab levels. Based on our studies, we expect to monitor subjects for molecular evidence of response to conatumumab in addition to an apparent clinical effect.

MATERIALS AND METHODS

In Vitro Assays

The human colorectal (CRC) cell line Colo205 was obtained from American Type Culture Collection (ATCC, Manassas, VA). Cells were grown as a monolayer in RPMI 1640 supplemented with 10% FBS and 1x L-glutamine.

Biotinylated conatumumab was mixed with Avidin D (Vector Laboratories, Burlingame, CA) at a 1:2 Avidin D:biotin-conatumumab molar ratio for 20 min at ambient temperature prior to treating the cells at 37°C for 2 h. Colo205 cells were harvested and fixed in 10% neutral buffered formalin (Sigma-Aldrich, St. Louis, MO) for 20 min at ambient temperature. Fixed cells were transferred to a 96-well plate (Costar[®]) at a density of 20,000 cells/well. Samples were incubated with 100 μ L of blocking buffer (1%BSA/0.2%Triton X-100/5% normal goat serum/PBS) for 30 min at ambient temperature. Primary antibodies, cleaved caspase-3 (1:200 v/v; Cell Signaling Technology cat#9661L, Danvers, MA) or M30 CytoDEATH[™] (1:100 v/v; Axxora LLC cat#ALX-804-590, San Diego, CA), were added to designated wells and incubated overnight at 4°C. The samples were washed twice in wash buffer (1%BSA/PBS) and then secondary antibodies, goat anti-rabbit IgG Alexa Fluor 647 (1:666 v/v; Invitrogen, Carlsbad, CA), or goat anti-mouse IgG Alexa Fluor 488 (1:666 v/v; Invitrogen) were added to the appropriate wells and incubated for 1 h in the dark at ambient temperature. The wells were washed twice in wash buffer, and samples were counterstained with 100 μ L/well of DAPI (2 μ g/mL in PBS; EMD Chemicals, Gibbstown, NJ) for 30 min in the dark at ambient temperature prior to imaging.

Measurement of Conatumumab Occupancy on Colo205 Cells

To assess conatumumab occupancy prior to initiating cell death, Colo205 cells were treated with Avidin D:biotin-conatumumab complexes for 20 min at ambient temperature. Cells were treated for a short length of time to avoid inducing cell death and under-representing receptor occupancy. Cells were harvested and incubated (500,000/well) for 30 min at 4°C with 1 μ g of PE-conjugated DR5 antibody (Amgen Inc.), or with 0.125 μ g anti-DR5-PE (eBiosciences cat#12-9908, San Diego, CA). Cells were washed and then analyzed by flow cytometry using a FACSCalibur (Becton Dickinson Immunocytometry Systems) with CellQuest (version 3.3).

Colo205 Xenograft Model

All procedures conducted on mice were conducted according to the guidelines of the Amgen Institutional Animal Care and Use Committee in compliance with the U.S. Public Service Policy of Humane Care and Use of Laboratory Animals. The laboratory holding the animals met all specifications of the Association for Assessment and Accreditation of Laboratory Animal Care.

Colo205 cells (2×10^6 with Matrigel at a ratio of 2:1) were injected subcutaneously in the flank of 5-to-6-week-old female CD1 *nu/nu* mice (Charles River Laboratories, Raleigh,

NC) ($n = 10$ per group), as described previously (19). Conatumumab or hFc (30 μg) was administered by intraperitoneal (i.p.) injection to mice bearing palpable tumors of approximately the same size ($\sim 400\text{--}500\text{ mm}^3$ as judged by visual assessment). Tumors were sampled via FNA after 24 h of treatment. Briefly, a small incision was made in the skin above the tumor, and the FNA was extracted using a 24 gauge \times 4 inch Chiba needle (thin walled flexible FNA needle) (Becton Dickinson, Franklin Lakes, NJ). The sample was transferred into a 2 mL vial containing 1.5 mL of 4% paraformaldehyde. An additional cytology smear was prepared by spreading cells onto a clean glass slide and staining with Diff-Quik. Subsequent FNA studies (not presented here) used 22 gauge needles without a skin incision, to more closely mimic clinical practice, and resulted in comparable yield and quality. The tumor was then excised, fixed in zinc formalin fixative (Z-Fix, Anatech Ltd, Battle Creek, MI), processed, and embedded in paraffin. Serum was also collected from each mouse at the time of tumor harvest.

Collection of Human FNA Samples

Mock FNAs were performed on freshly resected human CRC tumors, obtained from Asterand (Detroit, MI) and Bio-Options (Fullerton, CA) within 18 h of surgery. Mock FNAs were collected from CRC tumors using a 22 gauge \times 6 inch Chiba needle (Becton Dickinson, Franklin Lakes, NJ) attached to a 12-mL syringe, and samples were deposited into a 2-mL Sarstedt tube containing 1.5 mL 4% paraformaldehyde. The tubes were gently inverted five times to adequately suspend the cells, and samples were stored at 4°C. A cytology smear was prepared as described above. Clinical FNAs from nonsmall cell lung cancer (NSCLC) patients were shipped in 2% formaldehyde at 4°C. All clinical trial procedures were reviewed and approved by internal and external Institutional Review Boards and conducted in accordance with the Declaration of Helsinki and the International Conference on Harmonization Good Clinical Practice guidelines.

Immunohistochemical Staining of Tumor Sections

Deparaffinized tissue sections were blocked (CAS BLOCK, Zymed Laboratories, San Francisco, CA) and incubated with rabbit polyclonal anti-cleaved caspase-3 antibody (1:200 v/v; Cell Signaling Technology, Danvers, MA). Tissue sections were quenched with peroxidase blocking solution (Dako Corp., Carpinteria, CA). The antibody was detected with an anti-rabbit HRP-conjugated antibody (Jackson ImmunoResearch Laboratories, West Grove, PA). Reaction sites were visualized with the 3'-diaminobenzidine tetrahydrochloride (DAB) + Substrate-Chromagen System (Dako Corp. Carpinteria, CA) and counterstained with hematoxylin.

Immunocytochemical Staining of FNAs

Fixed FNA samples were gently resuspended by pipetting, washed twice with PBS, and cytocentrifuged at 55g (700–900 rpm; Shandon cytopspin 4, Thermo Fisher Scientific, Fremont, CA) onto slides. The cytopspots were incubated for 30 min with blocking buffer (PBS/1% BSA/5% normal goat and horse

serum). Slides were incubated overnight with 100 μL of PBS-1% BSA containing 0.25 $\mu\text{g}/\text{mL}$ mouse anti-EpCAM monoclonal antibody (Cell Signaling Technology cat#2929, Danvers, MA) at 4°C. After washing twice in PBS-BSA, slides were incubated overnight at 4°C with 100 μL of PBS-BSA containing 0.2% Triton X (PBS-BSA-TX) and either anti-caspase-3 antibody (1:200 v/v, Cell Signaling Technology, Danvers, MA) or with anti-caspase-3 plus a twofold volume excess blocking peptide (Cell Signaling Technology, Danvers, MA). After two washes, slides were incubated with 100 μL of PBS-BSA containing secondary antibodies conjugated to Alexa Fluor 488 (goat anti-mouse IgG) and Alexa Fluor 633 (goat anti-rabbit IgG; Invitrogen, Carlsbad, CA) at a 1:666 dilution in PBS-BSA for 1 h in the dark at ambient temperature. Samples were incubated in 100 μL Hoechst 33342 (2 $\mu\text{g}/\text{mL}$; Invitrogen, Carlsbad, CA) for 10 min in the dark at ambient temperatures to stain for DNA. Stability of activated caspase-3 was studied in treated colo205 cells stored in 10% neutral buffered formalin. Cells were stained periodically over 4 months with no observed change in the percentage of cells containing activated caspase-3 (mean 90.77%, SEM 1.00, 95% CI [86.46, 95.08], 1.91% CV).

Image Acquisition and Quantitation

Xenograft sections. Images (20 \times) from tumor areas that were positively stained for active caspase-3/DAB were captured and quantified using an iColor Laser Scanning Cytometer (CompuCyte Corporation, Cambridge, MA) equipped with 440 nm, 532 nm, and 633 nm lasers, paired photomultiplier tubes (filters 490/40, 675/50, 650/LP), and associated software (v3.2.5). The low- and high-resolution images were captured using 20 μm and 0.5 μm scan step sizes, respectively. The area of the tumor positive for caspase-3/DAB was quantified by overlaying a lattice of circular contours (radius = 10 μm). During analysis, digital tissue maps were restricted by gates to exclude necrotic foci and non-tumor tissue (skin, capsule, etc.). Gating regions were defined on histograms or scatter plots (440 Invert Integral vs. 663 Invert Integral) to uniformly distinguish positively stained DAB events from negative events. These gated events were verified as DAB positive using image relocation galleries.

FNA samples. Cytometric measurements were performed using an iCys Laser Scanning Cytometer (CompuCyte Corp., Cambridge, MA) equipped with 405 nm, 488 nm, and 633 nm lasers and paired PMTs with filters (450/40, 530/30 and 650/LP) and associated software (v3.2.4). Low (20 μm scan step size) and high (0.5 μm scan step size) resolution scans were performed using 20 \times and 40 \times objectives, respectively. Events were contoured based on a nuclear stain threshold, and cytoplasmic staining was defined at a 4 pixel distance from the threshold contour. Large clumps of cells were excluded from analysis. The gating regions for the activated caspase-3-positive population were established based on the staining control samples (secondary antibody alone and/or peptide-blocked primary antibody). The integrity of the population was

verified by relocating positive events into an image gallery and visually confirming the morphology of positively stained cells. Apoptotic debris was excluded from sample analysis, because the sub-G1 peak biased the cell count and skewed the apparent percentage of caspase-positive cells. The “sub-G1” peak is comprised of multiple apoptotic bodies and chromatin fragments from a single apoptotic cell. Therefore, as suggested by others, this fractional DNA content should be excluded from the calculation of an apoptotic index (29).

Serum Assays

Levels of serum conatumumab were measured as described elsewhere (19).

Caspase-3/7 activity in mouse sera was determined using the Caspase-Glo[®] 3/7 Assay (Promega Corp., Madison WI). Mouse sera were diluted to 25% in Promega Caspase-Glo[®] Buffer and added to wells of a 96-well microtiter plate (Black/White Isoplate-96, PerkinElmer Inc., Waltham MA). An equal volume of Caspase-Glo[®] 3/7 substrate was added, plates were incubated at 30°C for 90 min, and then the luminescence from each well was read using the PerkinElmer EnVision plate reader (PerkinElmer Inc., Waltham, MA).

Statistical Analysis

Statistical analysis was done using SAS version 9.1. Significance was evaluated at $\alpha = 0.05$, and data were transformed to meet the normality assumption. Correlation between sample types was determined with a mixed effect model, which included treatment as a fixed effect and assumed within donor correlation was fit to appropriately transformed results for each sample type (log transformation for FNAs and tissue sections and inverse transformation for serum caspase activity). To assess procedural variability, a mixed effect model was used that included dose as a fixed effect and staining replicate as a random effect and was fit to the log-transformed data.

RESULTS

Induction of Caspase-3 Activation by Cross-Linked Conatumumab in Colo205 Cells

In previous studies, the proapoptotic activity of conatumumab was established in multiple tumor cell lines by measuring the activity of caspases in lysates using a peptide substrate (19). However, FNA biopsies yield small amounts of tumor cells and are not well suited for this lysate analysis. Consequently, we tested conatumumab potency in fixed but intact Colo205 cells by measuring a specific neo-epitope exposed on activated caspase-3 (Fig. 1). Consistent with our previous report, conatumumab required crosslinking to induce death *in vitro*. Detection of activated caspase-3 and its cytokeratin cleavage product, M30, were maximally observed at 1 $\mu\text{g}/\text{mL}$ biotin-conatumumab and required the presence of avidin (Fig. 1A). Caspase-3 activation increased with time, and was detected in ~75% of cells after 120 min (Fig. 1B). The kinetics of M30 detection were similar, albeit in a smaller percentage of cells (data not shown). To demonstrate occupancy of DR5 by conatumumab, drug-competitive and non-

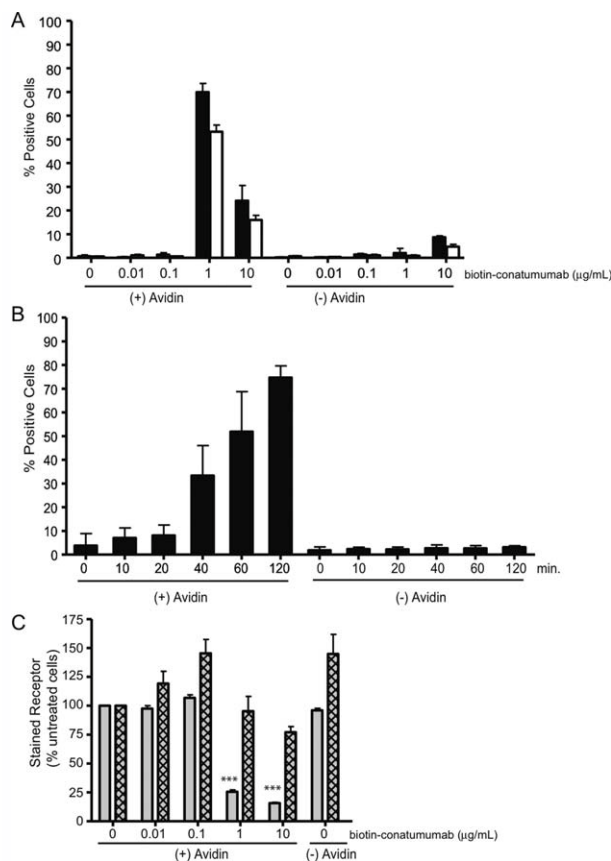


Figure 1. Caspase-3 activation in intact tumor cells. Colo205 cells were treated with biotin-conatumumab at the indicated concentrations \pm avidin for 2 h (A) or with 1 $\mu\text{g}/\text{mL}$ biotin-conatumumab for the indicated times (B). Activity was measured by laser scanning cytometry and expressed as mean percent of cells positively stained for either activated caspase-3 (solid bars) or M30 (open bars) \pm SD. (C) Conatumumab occupancy on Colo205 cells was measured by flow cytometry using other DR5 antibodies that were either strongly competitive with conatumumab (grey bars) or weakly competitive with conatumumab (hatched bars). Data are expressed as mean percentage of untreated cells \pm SEM, and are representative of at least 3 independent experiments. Significant changes ($P < 0.001$, ANOVA) from 0 $\mu\text{g}/\text{mL}$ (+) avidin control are indicated by ***. Changes observed with the weakly competitive antibody were not significant ($P > 0.05$). Analysis of receptor occupancy data using mean fluorescence intensity was comparable (Supporting Information Fig. 1).

competitive anti-DR5 antibodies were incubated with conatumumab-treated cells (Fig. 1C). Total DR5 levels remained unchanged at 1 $\mu\text{g}/\text{mL}$ of conatumumab, but only ~18% of Colo205 cells had available receptor to bind the conatumumab-competitive antibody. Taken together these data confirmed that immunodetection of caspase-3 activation in intact cells is a practical marker of on-target activity for conatumumab, and suggested that the LSC approach may be suitable for whole cell analysis in FNAs.

Caspase-3 Activity in Fine Needle Aspirates

Next, we assessed caspase-3 activation in FNAs prepared from mouse xenograft tumors. Increased caspase-3 activation

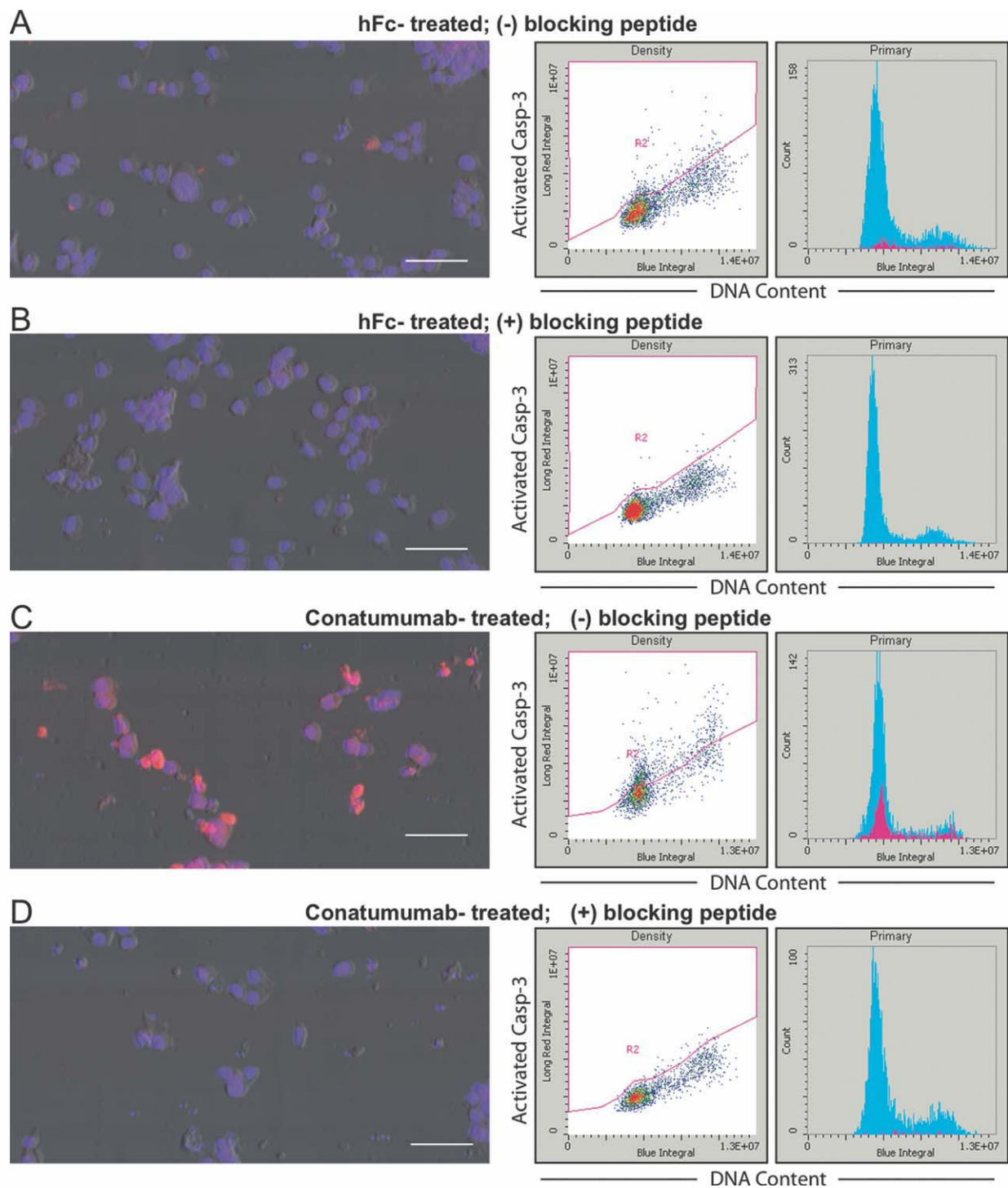


Figure 2. Conatumumab-induced caspase-3 activation in fine needle aspirates. FNAs were collected from Colo205 tumor-bearing mice 24 h after a single dose of 30 μg of control human (h)Fc (**A, B**) or conatumumab (**C, D**). Representative image fields of samples stained with anti-activated caspase-3 (red) and Hoechst (blue) are shown. Laser scanning cytometry analysis was restricted to single cells based on the DNA profile (blue integral), and the R2 caspase-positive gate (long red integral) was established from sample-matched blocking peptide controls (**B, D**). Scale bar = 50 μm .

was detected in tumor FNAs prepared from conatumumab-treated mice, as compared with control human Fc-treated mice (Figs. 2A and 2C). The specificity of detection was con-

firmed by including a blocking peptide that abrogated the caspase-3 signal (Figs. 2B and 2D). Cytometric quantitation was performed by using DNA content information to restrict

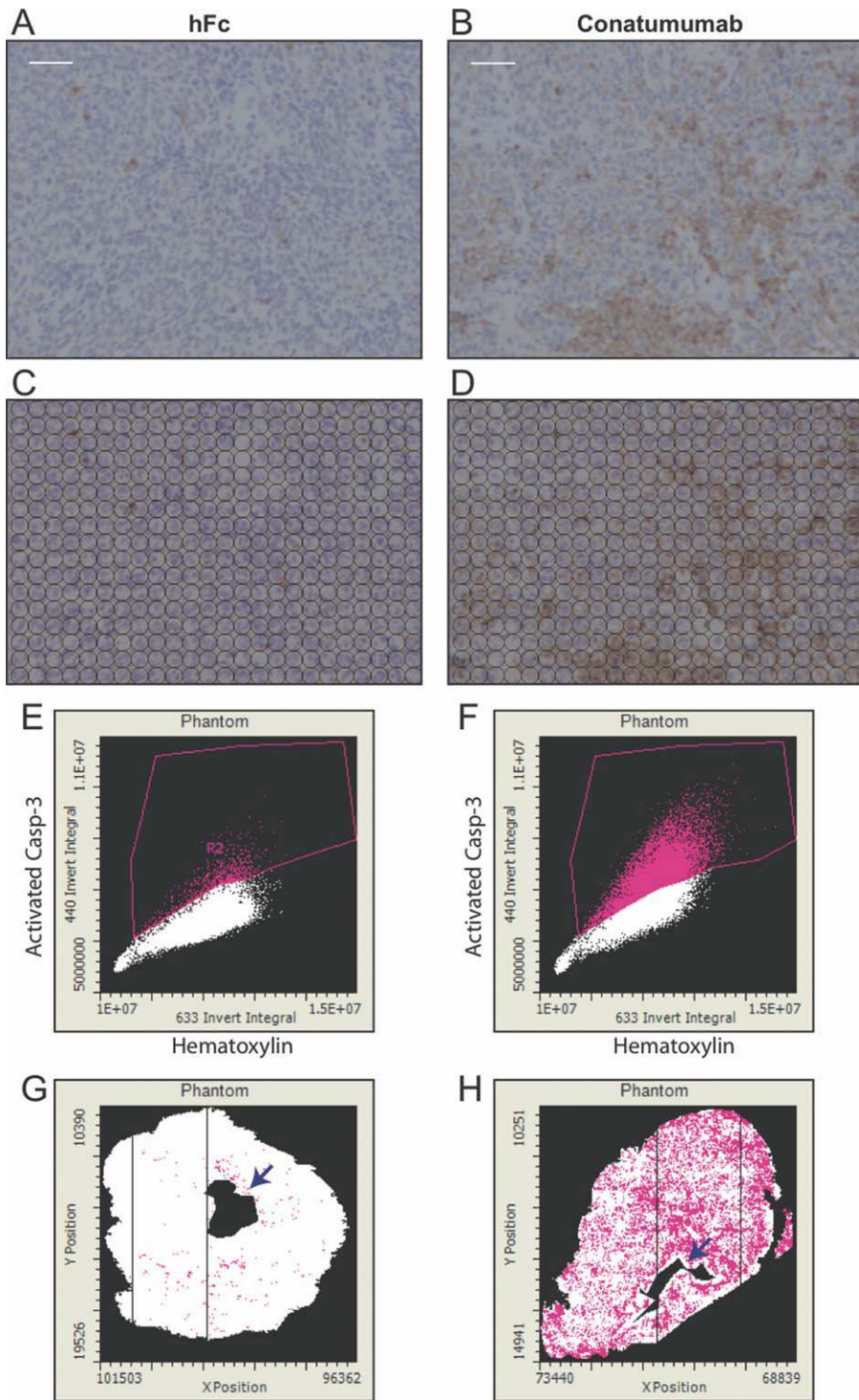


Figure 3. Conatumumab-induced caspase-3 activation in xenografts. The area of tumor section positively stained by DAB for activated caspase-3 was assessed by laser scanning cytometry. Panels **A, C, E, G** correspond to a representative xenograft section from an hFc-treated animal, whereas panels **B, D, F, H** correspond to a conatumumab-treated animal. Scale bar = 50 μ m. (C, D) Image analysis involved stereologic sampling of fields with a lattice of circular contours. Images were pseudocolored to depict blue hematoxylin and brown DAB staining for purposes of presentation only; quantitation was performed using monochromatic channels. (E, F) Each circular contour was plotted as a function of its integral laser light absorption in the DAB (440 nm absorption) and hematoxylin (633 nm absorption) channels. Gating regions were used to distinguish positively stained DAB events (magenta) from negative events (white). Gated events were verified as DAB positive using image relocation galleries. (G, H) Positive events were mapped as a function of their x/y coordinates to reconstruct staining distribution. Arrow indicates the hole left by FNA sampling prior to embedding.

analysis to single cells (Fig. 2). A caspase-3 positive threshold was set for each animal based on the blocking peptide control, such that fewer than 2% of cells were positive in the blocking peptide sample. Interestingly, caspase-3 activation was observed at all phases of the cell cycle.

The feasibility of using FNAs to sample the overall pharmacodynamic impact of conatumumab was assessed in mice

by comparing levels of activated caspase-3 in FNAs to levels of activated caspase-3 in xenograft sections and levels of activated caspase-3/7 in serum. The area of tumor section positively stained for activated caspase-3 was determined in xenograft sections from the same tumors that were sampled by FNA. Sections of formalin-fixed paraffin embedded xenografts were chromatically stained for activated caspase-3 (Figs. 3A and 3B),

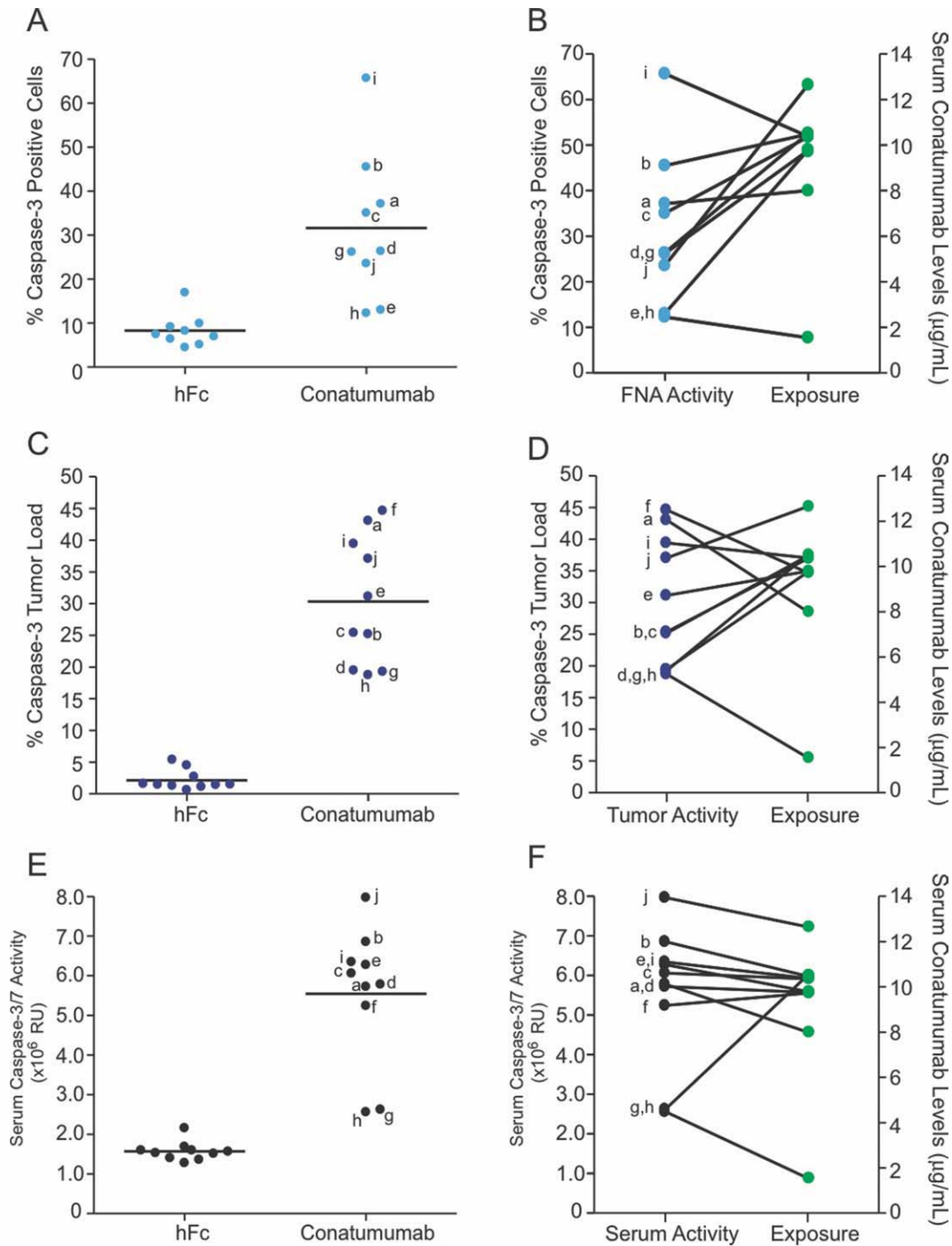


Figure 4. Comparison of sampling methods for tumors and serum. (A) The mean percentage of caspase-3 positive cells in replicate FNAs (2-3) were calculated for each hFc or conatumumab treated mouse. Group mean values are designated by the horizontal line. (C) The area of tumor section positively stained for activated caspase-3 (% Caspase-3 Tumor Load = $100 \times$ area of DAB stained section/total area of tumor section) was calculated from the resected tumor for each mouse. (E) Serum levels of caspase-3/7 activity were measured in relative light units (RU) for each mouse. Lower case letters (a-j) identify individual mice across assay platforms. (B, D, F) Caspase activation in each sample type was correlated to serum levels of conatumumab.

and caspase-3 tumor load was quantitated by LSC using a stereological sampling method (Figs. 3C–3H). All sample types demonstrated a treatment effect when comparing mice dosed with conatumumab ($n = 10$) to mice dosed with con-

trol human Fc ($n = 10$) (FNAs $P = 0.0001$; sections and serum caspase-3/7 activity $P < 0.0001$) (Figs. 4A, 4C, and 4E). The correlation between the percentage of activated caspase-3 positive cells in FNAs and activated caspase-3 in sections was

significant at $\alpha = 0.05$ significance level when evaluated using Spearman's ρ correlation ($P < 0.0001$). Similarly, the correlations between serum caspase-3/7 activity and activated caspase-3 in sections or FNAs were also significant at $\alpha = 0.05$ significance level ($P < 0.0001$). Confirming the link between effect and exposure, serum concentration of conatumumab correlated significantly with activated caspase-3 in FNAs (Fig. 4B) when evaluated using Spearman's ρ correlation ($P < 0.0001$). Serum conatumumab levels also correlated with activated caspase-3 in tumor sections ($P < 0.0001$, Fig. 4D) and with serum caspase-3/7 activity ($P < 0.0001$, Fig. 4F). There was one animal in the hFc group and one animal in the conatumumab group that did not yield a useable FNA, but for which section and serum data were collected. Data from these animals were excluded from the correlation analysis across sample type.

Characterization and Implementation of a Multiplexed Assay for Clinical Specimens

To establish the assay performance parameters prior to clinical implementation, we thoroughly assessed the variability and relative specificity of the FNA staining assay. Colo205 cytopspot samples contained a baseline level of activated caspase-3 (mean 11.80%, SEM 1.21, 95% CI [6.57, 17.03]), which dramatically increased in conatumumab-treated Colo205 cells (mean 63.59%, SEM 6.84, 95% CI [34.18, 93.00]) (Fig. 5A). The precision of triplicate measurements for conatumumab-treated and nontreated cells was 17.86% and 18.62% CV, respectively. Staining specificity was confirmed by including an epitope peptide that blocked caspase-3 immunodetection to levels observed with the secondary antibody alone (peptide-blocked: mean 1.54%, SEM 0.47; secondary alone: mean 1.16%, SEM 0.31). In contrast, an unrelated peptide did not affect detection of activated caspase-3 in conatumumab-treated samples (mean 72.76%, SEM 2.50) or non-treated samples (11.37%, SEM 1.34). Using a mixed effect model, statistical analysis of these data indicated that staining variability accounted for only 2–3% of the total variability in samples stained for activated caspase-3 (Supporting Information Table 1).

To estimate the baseline level of activated caspase-3 in human tumors, mock FNAs were prepared from 3 resected human CRC samples (Fig. 5A). The percentages of cells containing baseline activated caspase-3 from CRC samples (mean 10.41%, SEM 0.85; mean 9.25%, SEM 0.85; mean 9.21%, SEM 0.64) were comparable to those of untreated Colo205 cells. A mixed effect model that included inter-patient, staining replicates within patient (intra-patient), repeat image acquisition on the same instrument, and the interaction between analysis and staining within patient as random effects was fitted to the log-transformed data. The total variability was 0.167 with 67% contributed by patient variability, 2% contributed by image acquisition variability, and 30% contributed by staining variability.

Because of the cellular heterogeneity commonly observed in actual clinical FNA samples, it was necessary to multiplex the assay with a marker for tumor cells, and epithelial cell

adhesion molecule (EpCam) was used for this purpose. Colo205 cells were spiked into peripheral blood mononuclear cells (PBMCs) and immunostained for EpCam along with a DNA marker (Fig. 5B). The Colo205 cells were readily distinguished from the PBMCs on the basis of EpCam signal intensity and DNA content analysis (Fig. 5C).

Giemsa staining confirmed that NSCLC clinical FNA samples contained tumor cells, but were variable in cellular composition (Figs. 6A and 6B). Laser scanning cytometry analysis of fluorescently stained samples from the same FNA helped resolve cell composition. EpCam positive cells within these clinical specimens were aneuploid and distinguishable from the nontumor cells (Figs. 6C and 6D). A small population of the EpCam positive cells was positive for activated caspase-3 (~2%) in the absence of therapy (Figs. 6E and 6F). Taken together, these data indicate that testing FNAs for caspase-3 activation in tumor cells is a viable approach to survey the pharmacodynamic activity of conatumumab in target tissues.

DISCUSSION

Detection of activated caspase-3 by immunohistochemical staining of tumor tissue provides a sensitive method for detection of apoptosis in situ, and may provide important evidence to support pharmacodynamic activity in early clinical trials of apoptosis-inducing drugs. Slide-based cytometry of immunostained FNAs is emerging as an application to help clinicians better understand patient populations and the impact of drugs (30–36). Two key advantages to this approach include the detection of on-target activity in small amounts of tumor tissue, rather than in peripheral surrogate compartments (e.g. blood or serum), and early evidence of drug activity prior to clinical signs of tumor regression. The challenge, however, is to establish a specific, sensitive, and quantitative assay that accommodates a viable biopsy method. Historically, this has not been easy to accomplish, and many approaches that showed promise in cell systems or animal models often failed in human studies (37–39). We describe here, preclinical and clinical implementation of a novel cytometric imaging assay that measures activated caspase-3 in FNAs.

Cell-culture experiments using similar concentrations of conatumumab as previously described (19) confirmed that activated caspase-3 could be detected in intact Colo205 cells, as with lysate-based assays, and that crosslinking of conatumumab was required for potency. We also investigated the appearance of a downstream product of caspase-3. The cleavage product of cytokeratin, M30, was detected after avidin/biotin-conatumumab treatment, verifying that M30 is linked to caspase-3 activation in tumor cells (19,40). Interestingly, at 10 $\mu\text{g}/\text{mL}$ the majority of DR5 was bound by conatumumab, but levels of activated caspase-3 were lower than those attained with 1 $\mu\text{g}/\text{mL}$ conatumumab. This is likely an artifact caused by pre-assembled avidin-biotin-conatumumab complexes, since a hook-effect was not observed in a previous study in which Protein A was used as the crosslinking agent (19). However, it is also possible that excessively high doses of conatumumab may saturate the DR5 receptors in vitro in a

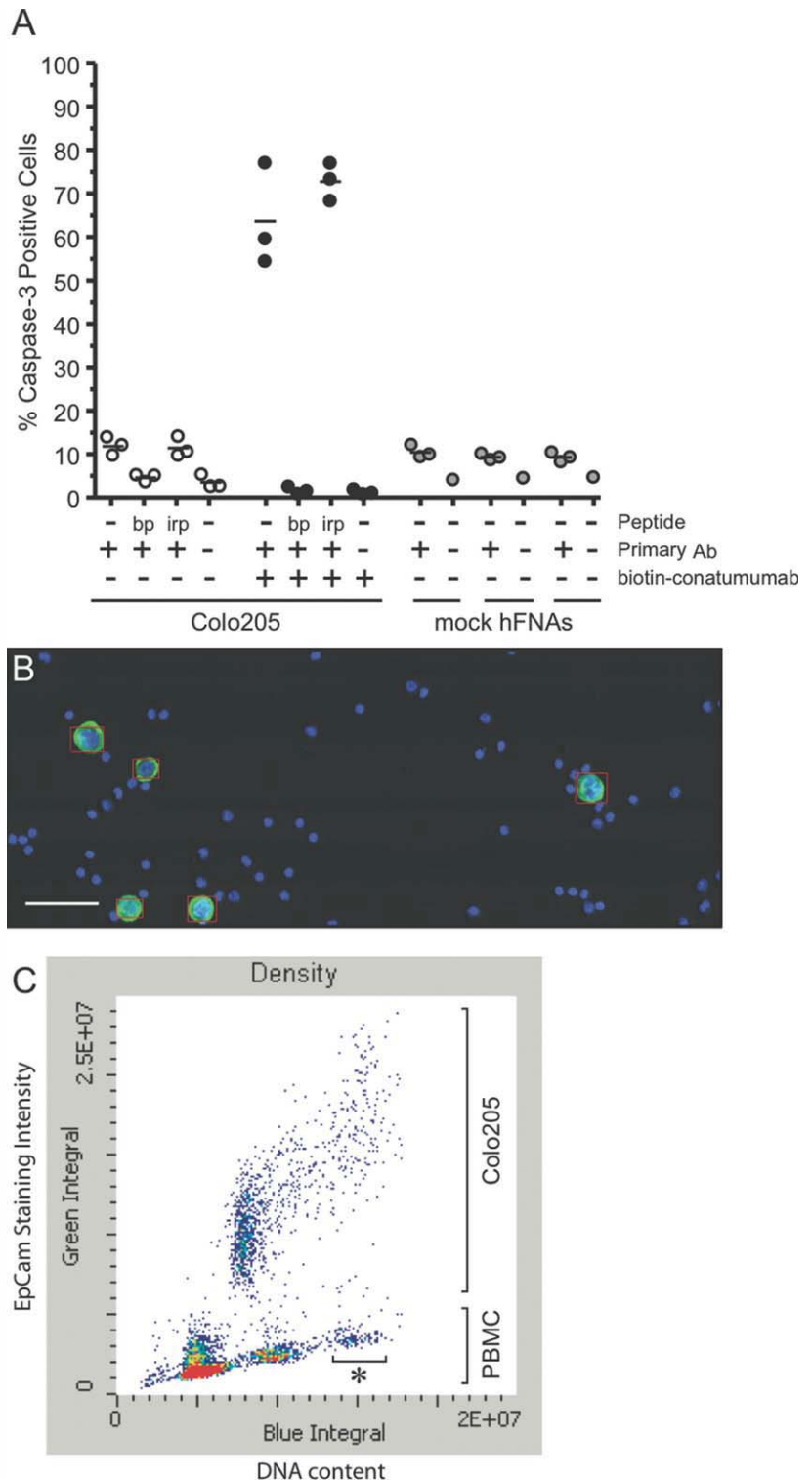


Figure 5. Optimization of FNA/LSC assay for use in the clinic. **(A)** Assay precision was measured using triplicate samples of untreated Colo205 cells (open circles), 1 $\mu\text{g}/\text{mL}$ avidin/biotin-conatumumab-treated Colo205 cells (black circles), or mock human FNAs (grey circles) prepared from three separate resected CRC tumors. Samples were also incubated with molar excess of epitope-blocking peptide (bp) or an irrelevant peptide (irp). **(B)** Colo205 cells were mixed with PBMCs, labeled with anti-EpCam, and analyzed by LSC. Scale bar = 50 μm . **(C)** EpCam staining intensity (green integral) was used to distinguish Colo205 cells from PBMCs. The DNA content (blue integral) of Colo205 cells as compared to PBMCs confirms the tetraploid property of these cells. Closely adjacent PBMCs were occasionally contoured together, which appears as a >G2M population that was EpCam negative (denoted by *).

manner that interferes with efficient receptor crosslinking or activation. Overall, these data support the hypothesis that conatumumab-induced caspase-3 activation can be adequately measured in intact cells, rather than relying on methods that disrupt the cell or that measure proteins released into the circulation by dying cells.

The assay was adapted to FNAs extracted from murine xenograft tumors by cytopinning the aspirate onto a slide and measuring the percentage of tumor cells containing activated caspase-3. Although the samples in this study were all collected in a terminal assay, we have begun to assess the value of longitudinal FNA sampling to reduce the number of animals

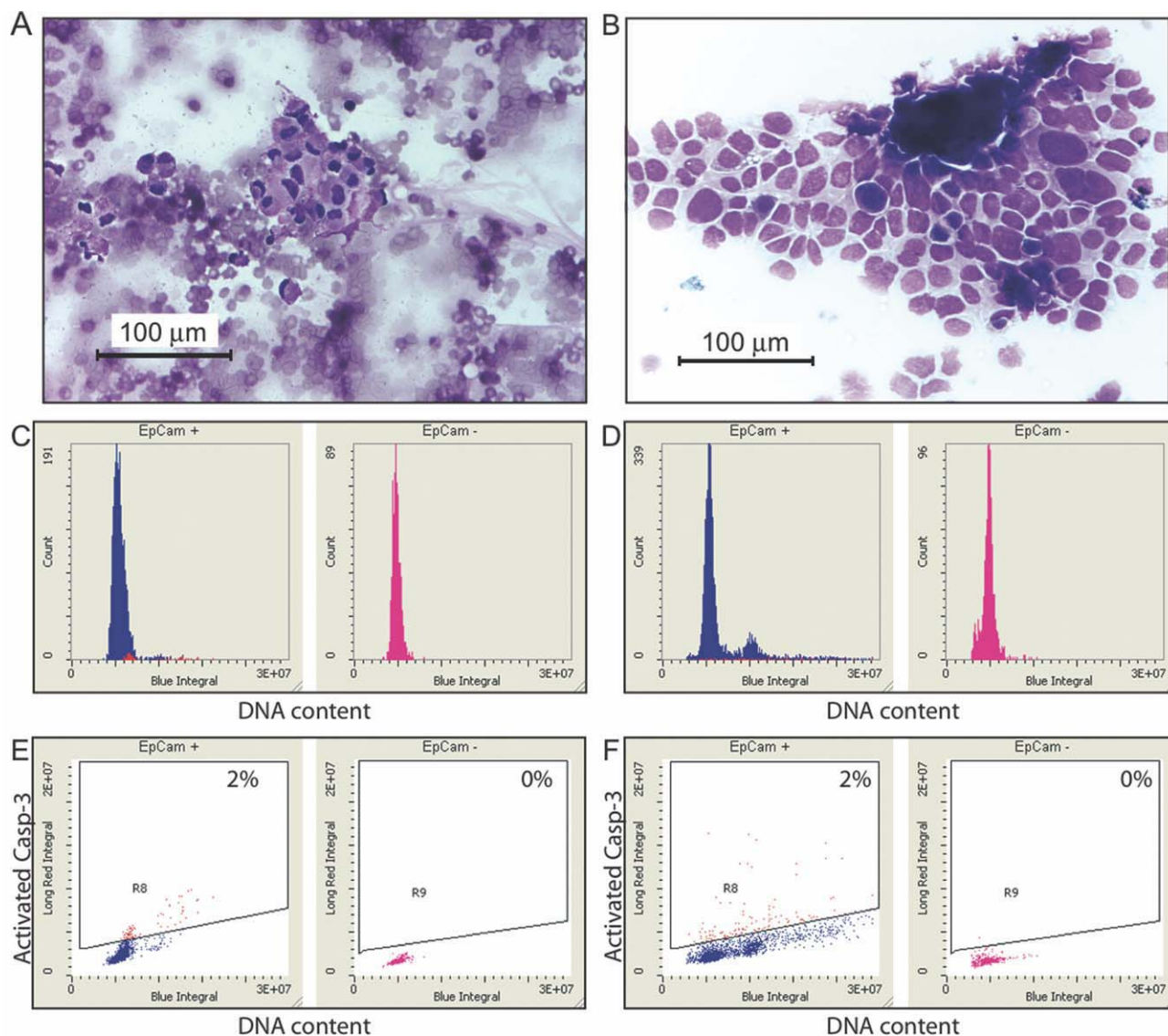


Figure 6. Cytometric analysis of clinical FNAs. (A, B) FNAs biopsied from metastatic lesions of 2 individuals with NSCLC were stained with Giemsa and imaged at $\times 20$ magnification using a Nikon FXA microscope equipped with a Nikon DXM1200 camera. (C, D) After immunofluorescent staining, EpCam positive and negative cells were analyzed from each patient for DNA content (Blue Integral). EpCam negative cells were predominantly in G1, consistent with growth arrested polymorphonuclear cells, and morphology was confirmed by image relocation (not shown). (E, F) Intensity of activated caspase-3 staining (long red integral) was expressed as a function of DNA content (blue integral). Activated caspase-3 gates were selected based on blocking peptide controls (as in Fig. 2) for EpCam positive tumor cells (R8) and EpCam negative (R9) nontumor cells. The percentage of cells that stained positive for activated caspase-3 is indicated for EpCam positive or negative subsets for each patient.

used in preclinical drug development, and to further emulate the clinical setting. We found that early caspase-3 activation (24 h after dosing with conatumumab), as measured by the percentage of activated caspase-3 positive cells in FNAs, correlated significantly both with the amount of activated caspase-3 measured within a tumor section (tumor load) and with serum caspase-3/7 activity. Since conatumumab does not bind detectably to mouse DRs, we reason that serum caspase-3/7 activity was derived from the implanted human tumor cells. This assumption, however, may not be as direct or valid when dosing humans, highlighting the value of clinical FNAs for quantitating in situ caspase activation.

A disadvantage of FNA sampling is that, in comparison with serum-based assays, the number of biopsies that can be acquired from an individual is very limited. Consequently, it is important to consider that an FNA will provide a single “snapshot” of a dynamic process occurring in vivo, where ongoing clearance of apoptotic cells from the tumor will likely confound absolute quantitation. Thus, the kinetics of drug mechanism should be considered prior to clinical implementation to inform sample collection time. Furthermore, to assess pharmacodynamic activity of conatumumab in humans, intra-patient pre and postconatumumab treatment FNAs should be compared. Therefore, we estimated intra-tumor

sampling bias by calculating the variability between preclinical FNA replicates from a single tumor. As indicated by the mixed effect model analysis of the FNA data, most of the variability was contributed by intra-animal (or intra-tumor) variation, suggesting that eight to ten replicates for each tumor would provide a reliable result. In clinical practice, this number of FNAs would not be feasible, and FNA sampling coupled with more sophisticated imaging techniques such as endoscopic ultrasound-guided or mammography-guided FNAs may be required to reduce variability (25,41). Further investigation on FNA collection methodology is underway to maximize the sampling area from a single FNA procedure.

Other highly sensitive methods to analyze FNA biopsies are also emerging, including a recent report using nanofluidic proteomics (42). These compelling approaches will likely provide value to clinical trials for patient stratification as well as the pharmacodynamic impact of drugs. The assay described here offers two distinguishing features that may be important to some clinical programs. First, the ability to partially deconvolute sample heterogeneity using tumor cell markers, such as EpCam (as described here) or cytokeratin (23), allows an investigator to restrict analysis to tumor cells and exclude stroma or cellular infiltrate, including white blood cells. Because clinical sample integrity can be highly variable in a multisite trial, enrichment for tumor cells during analysis may partially compensate for discrepancies in sample acquisition. In addition, the preservation of cellular integrity allows simultaneous DNA content analysis. By collecting the aspirates in suspension (2% p-formaldehyde) instead of embedding samples into a cell block, we avoid the need for processing and sectioning the sample. This enabled measurement of caspase-3 activation relative to the DNA profiles on a single-cell basis. We are currently using this same approach with FNAs to evaluate phosphorylated Histone H3 as an indicator of anti-mitotic therapy.

In summary, we have described a new cytometric approach to evaluate FNA biopsies for evidence of on-target activity from the apoptosis inducing drug, conatumumab. We demonstrated that this approach can be used preclinically to establish correlation with section-based and serum-based biomarkers prior to clinical implementation. Furthermore, we demonstrated that the approach can be successfully used to evaluate clinical specimens. Future work is focused on integrating this approach into a conatumumab clinical trial.

ACKNOWLEDGMENTS

The authors wish to acknowledge the encouragement, intellectual, and technical contribution provided by Ildiko Sarosi. They also wish to thank P. LoRusso for collection of clinical specimens, M. Peach and R. Manoukian for technical support, S. Patterson for helpful insight, J. Ferbas for program support, I. McCaffery for sharing commercially procured tumor samples, J. Wiezorek for oversight of clinical development, and K. Boorer for editorial assistance. All authors except R. Herbst are employees of Amgen, Inc. and own company stock/stock options, but do not directly financially benefit from the publication of these results.

LITERATURE CITED

- LeBlanc HN, Ashkenazi A. Apo2L/TRAIL and its death and decoy receptors. *Cell Death Differ* 2003;10:66–75.
- Pan G, O'Rourke K, Chinnaiyan AM, Gentz R, Ebner N, Ni J, Dixit VM. The receptor for the cytotoxic ligand TRAIL. *Science* 1997;276:111–113.
- Sheridan JP, Marsters SA, Pitti RM, Gurney A, Skubatch M, Baldwin D, Ramakrishnan L, Gray CL, Baker K, Wood WI, Goddard AD, Godowski P, Ashkenazi A. Control of TRAIL-induced apoptosis by a family of signaling and decoy receptors. *Science* 1997;277:818–821.
- Truneh A, Sharma S, Silverman C, Khandekar S, Reddy MP, Deen KC, McLaughlin MM, Srinivasula SM, Livi GP, Marshall LA, Alnemri ES, Williams WV, Doyle ML. Temperature-sensitive differential affinity of TRAIL for its receptors. DR5 is the highest affinity receptor. *J Biol Chem* 2000;275:23319–23325.
- Walczak H, Degli-Esposti MA, Johnson RS, Smolak PJ, Waugh JY, Boiani N, Timour MS, Gerhart MJ, Schooley KA, Smith CA, Goodwin RG, Rauch CT. TRAIL-R2: A novel apoptosis-mediating receptor for TRAIL. *EMBO J* 1997;16:5386–5397.
- Peter ME, Krammer PH. The CD95(APO-1/Fas) DISC and beyond. *Cell Death Differ* 2003;10:26–35.
- Kischkel FC, Lawrence DA, Chuntharapai A, Schow P, Kim KJ, Ashkenazi A. Apo2L/TRAIL-dependent recruitment of endogenous FADD and caspase-8 to death receptors 4 and 5. *Immunity* 2000;12:611–620.
- Lavrik I, Krueger A, Schmitz I, Baumann S, Weyd H, Krammer PH, Kirchhoff S. The active caspase-8 heterotetramer is formed at the CD95 DISC. *Cell Death Differ* 2003;10:144–145.
- Sprick MR, Weigand MA, Rieser E, Rauch CT, Juo P, Blenis J, Krammer PH, Walczak H. FADD/MORT1 and caspase-8 are recruited to TRAIL receptors 1 and 2 and are essential for apoptosis mediated by TRAIL receptor 2. *Immunity* 2000;12:599–609.
- Deng Y, Lin Y, Wu X. TRAIL-induced apoptosis requires Bax-dependent mitochondrial release of Smac/DIABLO. *Genes Dev* 2002;16:33–45.
- Suliman A, Lam A, Datta R, Srivastava RK. Intracellular mechanisms of TRAIL: Apoptosis through mitochondrial-dependent and -independent pathways. *Oncogene* 2001;20:2122–2133.
- Ashkenazi A, Holland P, Eckhardt SG. Ligand-based targeting of apoptosis in cancer: The potential of recombinant human apoptosis ligand 2/Tumor necrosis factor-related apoptosis-inducing ligand (rhApo2L/TRAIL). *J Clin Oncol* 2008;26:3621–3630.
- Pollack IF, Erff M, Ashkenazi A. Direct stimulation of apoptotic signaling by soluble Apo2L/tumor necrosis factor-related apoptosis-inducing ligand leads to selective killing of glioma cells. *Clin Cancer Res* 2001;7:1362–1369.
- Adams C, Totpal K, Lawrence D, Marsters S, Pitti R, Yee S, Ross S, Deforge L, Koepfen H, Sagolla M, Compaan D, Lowman H, Hymowitz S, Ashkenazi A. Structural and functional analysis of the interaction between the agonistic monoclonal antibody Apomab and the proapoptotic receptor DR5. *Cell Death Differ* 2008;15:751–761.
- Chuntharapai A, Dodge K, Grimmer K, Schroeder K, Marsters SA, Koepfen H, Ashkenazi A, Kim KJ. Isotype-dependent inhibition of tumor growth in vivo by monoclonal antibodies to death receptor 4. *J Immunol* 2001;166:4891–4898.
- Georgakis GV, Li Y, Humphreys R, Andreff M, O'Brien S, Younes M, Carbone A, Albert V, Younes A. Activity of selective fully human agonistic antibodies to the TRAIL death receptors TRAIL-R1 and TRAIL-R2 in primary and cultured lymphoma cells: Induction of apoptosis and enhancement of doxorubicin- and bortezomib-induced cell death. *Br J Haematol* 2005;130:501–510.
- Guo Y, Chen C, Zheng Y, Zhang J, Tao X, Liu S, Zheng D, Liu Y. A novel anti-human DR5 monoclonal antibody with tumoricidal activity induces caspase-dependent and caspase-independent cell death. *J Biol Chem* 2005;280:41940–41952.
- Kelley SK, Ashkenazi A. Targeting death receptors in cancer with Apo2L/TRAIL. *Curr Opin Pharmacol* 2004;4:333–339.
- Kaplan-Lefko PJ, Graves JD, Zoog SJ, Pan Y, Wall J, Branstetter DG, Moriguchi J, Coxon A, Huard JN, Xu R, Peach ML, Juan G, Kaufman S, Chen Q, Bianchi A, Kordech JJ, Ma M, Foltz IN, Gliniak BC. Conatumumab, a fully human agonist antibody to death receptor 5, induces apoptosis via caspase activation in multiple tumor types. *Cancer Biol Ther* 2010;9:616–629.
- LoRusso P, Hong D, Heath E, Kurzrock R, Wang D, Hsu M, Goyal L, Wiezorek J, Storgard C, Herbst R. First-in-human study of AMG 655, a pro-apoptotic TRAIL receptor-2 agonist, in adult patients with advanced solid tumors. *J Clin Oncol ASCO Annu Meeting Proc* 2007;25(18S):3534.
- Boeddinghaus I, Johnson SR. Serial biopsies/fine-needle aspirates and their assessment. *Methods Mol Med* 2006;120:29–41.
- Saleh H, Masood S. Value of ancillary studies in fine-needle aspiration biopsy. *Diagn Cytopathol* 1995;13:310–315.
- Brotherick I, Shenton BK, Lennard TW. Are fine-needle breast aspirates representative of the underlying solid tumour? A comparison of receptor levels, ploidy and the influence of cytokeratin gates. *Br J Cancer* 1995;72:732–737.
- Nizzoli R, Bozzetti C, Naldi N, Guazzi A, Gabrielli M, Michiara M, Camisa R, Barilli A, Cocconi G. Comparison of the results of immunocytochemical assays for biological variables on preoperative fine-needle aspirates and on surgical specimens of primary breast carcinomas. *Cancer* 2000;90:61–66.
- Kulesza P, Eltoum IA. Endoscopic ultrasound-guided fine-needle aspiration: Sampling, pitfalls, and quality management. *Clin Gastroenterol Hepatol* 2007;5:1248–1254.
- Schwock J, Ho JC, Luther E, Hedley DW, Geddie WR. Measurement of signaling pathway activities in solid tumor fine-needle biopsies by slide-based cytometry. *Diagn Mol Pathol* 2007;16:130–140.
- Zabaglo L, Ormerod MG, Dowsett M. Measurement of markers for breast cancer in a model system using laser scanning cytometry. *Cytometry* 2000;41:166–171.
- Zabaglo L, Ormerod MG, Dowsett M. Measurement of proliferation marker Ki67 in breast tumour FNAs using laser scanning cytometry in comparison to conventional immunocytochemistry. *Cytometry B Clin Cytom* 2003;56B:55–61.

29. Darzynkiewicz Z, Juan G, Li X, Gorczyca W, Murakami T, Traganos F. Cytometry in cell necrobiology: Analysis of apoptosis and accidental cell death (necrosis). *Cytometry* 1997;27:1–20.
30. Assersohn L, Salter J, Powles TJ, A'Hern R, Makris A, Gregory RK, Chang J, Dowsett M. Studies of the potential utility of Ki67 as a predictive molecular marker of clinical response in primary breast cancer. *Breast Cancer Res Treat* 2003;82:113–123.
31. Gerstner AO, Laffers W, Tarnok A. Clinical applications of slide-based cytometry—an update. *J Biophotonics* 2009;2:463–469.
32. Nizzoli R, Bozzetti C, Crafa P, Naldi N, Guazzi A, Di Blasio B, Camisa R, Cascinu S. Immunocytochemical evaluation of HER-2/neu on fine-needle aspirates from primary breast carcinomas. *Diagn Cytopathol* 2003;28:142–146.
33. Ostrowski ML, Pindur J, Laucirica R, Chakraborty S, Ramzy I. Proliferative activity in invasive breast carcinoma: A comprehensive comparison of MIB-1 immunocytochemical staining in aspiration biopsies to image analytic, flow cytometric and histologic parameters. *Acta Cytol* 2001;45:965–972.
34. Verstovsek G, Chakraborty S, Ramzy I, Jorgensen JL. Large B-cell lymphomas: Fine-needle aspiration plays an important role in initial diagnosis of cases which are falsely negative by flow cytometry. *Diagn Cytopathol* 2002;27:282–285.
35. Yoder M, Zimmerman RL, Bibbo M. Two-color immunostaining of liver fine needle aspiration biopsies with CD34 and carcinoembryonic antigen. Potential utilization in the diagnosis of primary hepatocellular carcinoma vs. metastatic tumor. *Anal Quant Cytol Histol* 2004;26:61–64.
36. Zimmerman RL, Logani S, Baloch Z. Evaluation of the CD34 and CD10 immunostains using a two-color staining protocol in liver fine-needle aspiration biopsies. *Diagn Cytopathol* 2005;32:88–91.
37. Baker M. In biomarkers we trust? *Nat Biotechnol* 2005;23:297–304.
38. Bakhtiar R. Biomarkers in drug discovery and development. *J Pharmacol Toxicol Methods* 2008;57:85–91.
39. Rifai N, Gerszten RE. Biomarker discovery and validation. *Clin Chem* 2006;52:1635–1637.
40. Biven K, Erdal H, Hagg M, Ueno T, Zhou R, Lynch M, Rowley B, Wood J, Zhang C, Toi M, Shoshan MC, Linder S. A novel assay for discovery and characterization of pro-apoptotic drugs and for monitoring apoptosis in patient sera. *Apoptosis* 2003;8:263–268.
41. Stomper PC, Budnick RM, Stewart CC. Use of specimen mammography-guided FNA (fine-needle aspirates) for flow cytometric multiple marker analysis and immunophenotyping in breast cancer. *Cytometry* 2000;42:165–173.
42. Fan AC, Deb-Basu D, Orban MW, Gotlib JR, Natkunam Y, O'Neill R, Padua RA, Xu L, Taketa D, Shirer AE, Beer S, Yee AX, Voehringer DW, Felsher DW. Nanofluidic proteomic assay for serial analysis of oncoprotein activation in clinical specimens. *Nat Med* 2009;15:566–571.